FIELD AND LABORATORY EXAMINATIONS OF AN ASR-AFFECTED BRIDGE – VARIATION IN CRACK EXTENT AND WATER CONTENT

Eva Rodum*, Bård M. Pedersen, Ragnhild Holen Relling

Norwegian Public Roads Administration, Trondheim/Bergen/Ålesund, NORWAY

Abstract

The Elgeseter bridge was built in Trondheim during the period 1949-1951. ASR damages were documented in the early 1990s and frequent examinations regarding rate of expansion and relative humidity, have been performed since 1995. The effect of both hydrophobic impregnation and Carbon Fiber Reinforced Polymer (CFRP) strengthening have been tested. Due to renovation works during the summer 2014-2015, the bridge was included as an object in an on-going R&D project. Crack widths were measured on selected columns and a large number of cores were drilled both from the columns and the bridge deck. The cores were subject to determination of the water content and internal cracking in the concrete.

The results from both previous (1995-2011) and the latest (2014-2015) examinations of moisture content and cracking on Elgeseter bridge are summarized in this paper.

Keywords: Alkali-silica reaction (ASR), concrete, bridge deck, bridge columns, crack extent, water content

1 INTRODUCTION

The Elgeseter bridge was built during the period 1949-1951 as a 200 m continuous concrete beam bridge with nine spans, each being 22.5 m long. Four 800x1450 mm² beams with center distance 5.5 m support the bridge deck and ø800 mm circular columns support the beams. The thickness of the bridge deck varies from 150-380 mm. The deck was cast monolithically with the beams, so were the beams and columns, except for the columns in axis 9. Each row of four columns has a 22 m long foundation beam, which is supported by 78 timber piles. Ice protection sleeves of 3 mm stainless steel are covering the lower 3 m of the columns. FIGURE 1 shows a cross section through the bridge deck and beams The axes are numbered 1-10, starting with the southern abutment (see FIGURE 13). The columns in each axis are numbered 1-4, starting with the western column (see FIGURE 14).

The ASR damages were diagnosed in 1990. Prior to this, closure of the deck joint in axis 10 and displacement of the top of the columns were observed. Since 1995, frequent examinations regarding rate of expansion (i.e. crack increase) and relative humidity have been performed. The effect of both hydrophobic impregnation (1995, 1999) and CFRP strengthening (2003) have been tested [1, 2]. The deformation of the columns in axes 7, 8 and 9 caused an overload situation and the columns were brought back into a perpendicular position in 2003. At the same time, the columns in axes 5-9 were coated with an elastic cement-based coating.

Due to renovation works during the summer 2014, the bridge was included as an object in the R&D project "Durable structures" (2012-2015) carried out by the Norwegian Public Roads Administration (NPRA). Crack widths were measured in the field and a large number of cores were drilled from both the columns and the bridge deck. The cores were subject to determination of the water content and internal cracking in the concrete. An overview of the internal cracking in the concrete bridge deck was needed for the structural evaluation of the superstructure during repair. Further, it was of general interest to extend the experience base concerning the relation between water content and degree of damage and the relation between external and internal cracking in ASR affected concrete.

2 THE CONCRETE COMPOSITION

Prior to the construction of the bridge, a comprehensive testing program was performed in order to achieve a concrete composition with sufficient compressive strength and durability properties [1]. Both frost deterioration and chloride induced reinforcement corrosion were addressed as potential problems. Based on results from freeze/thaw testing, an air volume of 4.2 % was aimed by adding air

* Correspondence to: eva.rodum@vegvesen.no

entrainment. In addition, marine (chloride infected) aggregates were avoided. ASR was, however, an unknown issue in Norway at that time, and the aggregates used were later revealed as highly alkali reactive. Glaciofluvial fine (0-16 mm) and coarse (15-35 mm) gravel were used in combination with crushed rock (3-15 mm). Micro structural analyses of the concrete revealed the following reactive rock types [1, 9]: Sandstone, greywacke, mylonite, phyllite, gneiss (finegrained), rhyolite, quartzite (fine grained), quartz rich rock and silt-claystone.

The need of a concrete compressive strength of 40 MPa in the columns led to the development of a project cement at Dalen Portland Cementfabrik AS. The cement (CEM I) was more fine grained and contained more gypsum than the normal standard cements at that time. The alkali content of the cement is unknown, but expected to be higher than 1 %. Based on given and estimated concrete recipes [1] the alkali content in the concrete is estimated to be approx. 4 and 5 kg/m^3 Na_2O_{eqv} for the beams/deck and columns, respectively.

3 EXAMINATIONS PERFORMED IN THE PERIOD 1990-2011

3.1 General

The ASR damages were diagnosed in 1990. Prior to this, closure of the deck joint in axis 10 (original opening 200 mm) and displacement of the columns (approximately 110 mm in axis 9 in 1991) were observed [3]. Photo of one of the columns in axis 9 (after repair of the columns in 2003), show the previous displacement of the column, estimated to approx. 150 mm in the longitudinal direction (FIGURE 10).

3.2 Columns

The columns are suffering from extensive cracking, mainly in the vertical direction. Earlier measurements of crack widths were performed in horizontal lines approx. 1 m above the ice protection sleeve (from boat), both in 1998 (all columns) and in 2011 (twelve columns in axes 2-4, those which were not coated in 2003)[4]. The width of each crack (cw) along the measuring line is measured, and a Surface Crack Index, SCI, is calculated according to Eq. (1)

$$SCI = \frac{\sum cw}{l} \qquad (1)$$

where l = length of the measuring line.

The results from the measurements in 1999 and 2011 are given in Table 1 and FIGURE 3. There is a clear tendency that the higher cracking intensity is measured on the western columns (number 1) and on the columns in the middle of the river (axes 5 and 6). The cracks are generally wider at the western sides of the columns, see example in FIGURE 2. In 1999, the SCI measured on the western columns varied from 1.8 to 4.5 ‰ with an average of 2.8 ‰. Further, there were no significant differences in SCI between the columns 2-4, here the SCIs measured in 1999 varied from 0.5 to 3 ‰ (all axes), with an average of 1.4 ‰. The expansion of the concrete have continued from 1999 to 2011, apparently most in the western columns. The increase in the SCI varied from 0.2 (note: surface treated columns in axis 2 not included) to 1.5 ‰ with an average of 0.8 ‰ (1.4 ‰ for C1 and 0.6 ‰ for C2-C4, respectively).

Jensen [4] performed measurements of expansion over single cracks and relative humidity in the concrete, in several locations on the bridge from 1995-2011. The expansion of cracks was measured by use of a DEMEC mechanical strain gauge. Three discs (measuring points) with internal distances of 50 mm were arranged in each location, two discs on the one side of the crack, one disc on the other. The wooden stick method [5] was used for measuring the relative humidity. Many of the measuring locations established by Jensen are potentially influenced by the hydrophobic impregnation and/or coating of the columns. As the effect of surface treatment is not a topic in this paper, only measurements in the period 1995-1998 are presented (before impregnation/coating).

Average RH values over four years (February 1995-December 1998), measured in four depths from the western surface (5, 25, 55 and 75 cm), are shown in FIGURE 4 (left) for column 1 and 4 in axis 2 and column 1 and 3 in axis 9. The RH is high, above 85 %, in all locations. The humidity is higher in the concrete exposed to the west compared to east and decreases from depth 5 to 75 cm for all columns. The average RH in the different depths from the western face is for the western columns (C1, which are most exposed to rain): 98.7, 97.5, 95.5 and 89.5 % and for the more sheltered columns (C3 and C4): 97.0 and 94.8 % (depths 5 cm and 25 cm, respectively).

The increase in single crack widths varies a lot between the different locations and over time. FIGURE 4 (right) show the crack increase in the same locations as the RH measurements (column 1 and 4 in axis 2 and column 1 and 3 in axis 9), over the same period (February 1995-December 1998).

Based on the plotted crack increase and slope of trend lines, the expansion rate may be divided into two main groups: The highest expansion rate (approx. 0.4 mm/4 years) is measured on the rain-exposed faces of both western columns and on the eastern face of one of the western columns (C1 in axis 2). The lowest expansion rate (approx. 0.1 mm/4 years) is measured on the western face of the sheltered columns (C3 and C4) and on the eastern face of one of the western columns (C1 in axis 9). Except for the behavior of the eastern face of the western column in axis 2, the correlation between measured RH and increase in crack widths seems good.

3.3 Beams and bridge deck

The bridge deck has by standard routine been visually inspected from beneath (underside), without showing typical ASR crack patterns. No detailed examination of the concrete in the deck were performed until 2014.

The beams have been under supervision due to ASR since 1990. The western beam between axes 1 and 2 (western face) was instrumented in one location by Jensen [4] in 1995, for measuring of relative humidity and expansion (changes in crack widths). The results from measurements over the period 1995-2011 are shown in FIGURE 5. The RH has increased over the years from 88/92 % to 95/100 % in depths 5/25 cm from the surface. The expansion measurements show closing of the crack (-0.5 mm), but slightly increased shear movement along the crack (0.26 mm).

Analyses on thin sections and plane-polished sections were performed in 1991 and 2012, showing a heavier extent of ASR in the western beam compared to the mid beams (2 and 3) [3]. Visual inspections and measurements of crack widths on site in 2011 revealed, however, that the mid beams were suffering from the largest cracks, up to 6 mm wide. Structural evaluations carried out by SINTEF as part of the NPRA's R&D project show a complex causal relationship between these cracks and the load situation (including extra loads due to expansions) and the structural design of the superstructure [8].

4 EXAMINATIONS PERFORMED IN 2014-2015

4.1 General

During the summer periods in 2014 and 2015, the NPRA carried out renovation works at the Elgeseter bridge, including the following aspects:

- Strengthening of the columns in axes 3 and 4 with CFRP
- Strengthening of single mid beams with CFRP, between axis 3-4 and 6-7.
- Removal of asphalt, membranes and different protective layers on the concrete deck, removal of delaminated concrete, patch repair and adding of new membrane and asphalt layer.
- Removal of old pavements and rebuilding new and wider ones.

The contractor of the renovation works raised scaffoldings both around the actual columns and beneath the actual beams in order to get access for the strengthening operations (FIGURE 6). Further, the renovation work gave direct access to the concrete surface on top of the deck. This gave the R&D project an opportunity to perform on site crack measurements and drill cores for laboratory examinations [9]. Further work is going on in a SINTEF project [6] in order to quantify the internal cracking in plane-polished sections, estimate the alkali content in the concrete and find a direct relation between the measured DCS and RH in the drilled cores.

4.2 Columns

Three columns in axis 4, number C1, C2 and C4, were examined in 2014, approximately 4.5 m above the ice protection sleeve. Crack widths were measured in two levels, with internal distances 0.6-0.9 m, and cores were drilled for determination of internal cracking and moisture state. The cores were drilled from surfaces without cracks (see example in Figure 9), from western and eastern side of column 1, western side of column 2 and eastern side of column 4. Special care was taken when drilling the cores for examination of moisture state. Free water on the core surfaces were wiped off and the cores were wrapped with plastic immediately after drilling, this to prevent supply/loss of water during sampling.

The maximum crack widths were 4.0, 1.4 and 0.8 mm for column C1, C2 and C4 respectively. The surface crack indexes (average of two levels) were 3.1, 1.7 and 1.6 ‰, calculated according to Eq. (1). The average crack indexes were calculated separately for the two half circumferences (west, east) demonstrating the more extensive cracking on the western side, especially for the western column (C1: 5.4 vs 0.8 ‰, C2: 2.4 vs 1.0 ‰ and C4: 2.0 vs 1.2 ‰). The surface crack indexes are shown in FIGURE 7.

The water content was determined in approx. 5 cm slices successively split from the surface of the drilled cores. The slices were weighed immediately after splitting (w_1), then after submersion in water for 7 days (w_2) and drying at 105 °C for 7 days (w_3). The degree of capillary saturation, DCS, was calculated according to Eq. (2) [7].

$$DCS = \frac{w1 - w3}{w2 - w3} \qquad (2)$$

The results (FIGURE 8, right) show a slight increase in DCS from the western face to the highest levels (97.5 and 93.2 %) at a depth of approx. 125 mm, thereafter decreasing through the columns to approx. 70-75 % near the eastern surfaces.

Examinations of plane-polished sections were performed by subjective visual evaluation (no crack counting or image analyses). It was concluded that the internal cracking in the western side of column C1 and C2 is more pronounced than the cracking in the eastern side of column C4, corresponding with the DCS profiles [9]. The main crack formation is parallel to the surface. See photos in FIGURE 9.

Measurements of maximum crack widths on the western face of column 1 in axis 3 were performed from each scaffolding platform levels 1-6 (FIGURE 6), showing a decrease in max. crack width with increasing height above the protection sleeve (FIGURE 8, left).

4.2 Bridge deck

After removal of asphalt and membrane from the bridge deck in 2014, the concrete surface revealed clear signs of ASR damages. Fractured surfaces showed dense rims around the aggregate particles (FIGURE 11), and delamination were detected in some areas of the deck, especially near the bridge joint in the northern part of the bridge and close to the end beams (sidewalk areas).

The visual situation on the underside of the deck, with white precipitation on certain surfaces (FIGURE 10, left), indicated that the earlier extension of the pavements had punctured the membrane in the outer parts of the deck, leading to increased water ingress and leakages through the concrete.

It was decided to drill cores from different parts of the deck (see FIGURE 13-15), in order to document the spread in water content and crack extent over the whole deck.

The water content was determined in approx. 5 cm slices successively split from the top surface of the drilled cores. The DCS values were calculated according to Eq. (2). The results confirm the assumptions that the water content is very high (98-99 %) in the western part of the deck (location 1), higher than in the middle part (location 2). Further, the water content in location 2 increases from location A to C (A: 76-83%, B: 88-93 % and C: 97-98 % in depths 0-150 mm). See FIGURE 16. It should be noted that severe cracking in several cores might have led to extra water uptake in the cores during drilling, thus to some extent overestimating the water content.

The visual examinations of the plane-polished sections (see example in FIGURE 15, right) indicate that the internal crack extent corresponds with the water content. Based on subjective evaluations (no crack counting or image analyses), more intense cracking is observed in location 1 vs. 2 and in location C-2 vs. A-2/B-2. This also corresponds with the location of the largest delamination areas during patch repair, which was observed close to the joint in axis 10 (FIGURE 12). In addition to ASR, frost action may have contributed to the cracking in the concrete most exposed to water.

The compressive strength was determined on two cores from each of the locations A, B and C. The average value per location A, B and C was: 34.1, 44.5 and 31.9 MPa. The results are in accordance with the specified compressive strength (32 MPa).

5 DISCUSSIONS

Columns:

There is a good correlation between the water content in the concrete and the extent of cracking, both external and internal cracking. These observed correlations are in accordance with previous Norwegian investigations [10], where the relationship between the water content (DCS) and an internal Crack Index, calculated based on crack counting of plane-polished sections [11], was studied. About 115 structural members from bridges and dams were included, and the majority of the structures with pronounced ASR had a DCS above 90 %. The DCS versus crack index for 46 bridges is shown in Figure 17.

The increased water content in the western sides of the columns corresponds with the weather conditions, as the western faces are much more exposed to rainwater (and direct sun) than the eastern faces. Further, the western column are more weather-exposed than the more sheltered columns in axes 2-4.

There is a good correlation between the previous RH values (FIGURE 4) and the latest DCS values (FIGURE 8), concerning the shape of the profiles from west to east. However, no direct relation between the two set of moisture parameters is established, and there are some uncertainty factors linked to the wooden stick method after so many years in service. Work is going on at SINTEF [6] in order to establish a relation between RH (Vaisala sensors) and DCS values, based on direct comparison between the two methods on the concrete material from Elgeseter bridge.

Surface crack indexes (SCI) in 2011 were measured approx. 1 m above the ice protection sleeve while the SCIs in 2014 were measured approx. 4.5 m above (platform level 3). The SCI_{2011} for column C1, C2 and C4 in axis 4 was 3.9, 2.7 and 2.6 ‰, while the SCI_{2014} was 3.1, 1.7 and 1.6 ‰. The ranging of columns is the same, but the values are generally higher in 2011. Measurements of maximum crack widths on the column 1 in axis 3 show a decrease in max. crack width with increasing height above the protection sleeve. The different measuring height may therefore explain the higher SCI_{2011} than SCI_{2014}. Different personnel performing the two set of measurements may also have caused some variations in the results.

The SCI could be used to express the rate of expansion, assuming that the cracks are formed as result of expansion only. Norwegian aggregates are slowly reactive, and if we assume that the first cracks were visible after 15 years, in 1966, the average rate of expansion for all columns 1 (C1 axes 2-9) from 1966-1999 could be expressed as $SCI_{1999C1axes2\text{-}9avg}$/(1999-1966)= 0.084 ‰/year. The average rate of expansion for the rest of the columns (C2-C4) in axes 2-9 over the same period would then be 0.042 ‰. To compare the rate of expansion in the periods 1966-1999 and 1999-2011, the results from axes 2-4 should be isolated (these were the only ones measured in 2011). The average rate of expansion for the columns 1 (C1) in axes 2-4 from 1966-1999 and 1999-2011 would then be 0.070 and 0.117 ‰/year, respectively, while the average rate of expansion for the other columns (C2-C4) in axes 2-4 over the same two periods would be 0.034 and 0.056 ‰/year. These calculations indicates a considerable increase (approx. 65 %) in the expansion rate the later years. The measured increase in crack widths may, however, for the larger cracks be influenced by other mechanisms, e.g. changes in geometry of the cracks (if for instance delamination in the bottom of the crack), frost action or reinforcement corrosion.

Bridge deck:

As for the columns, there is a good correlation between the water content in the concrete and the extent of internal cracking. The increased damage extent (water content/cracking) in location 1 may be explained by the damages on the membrane caused by extending the pavements in 1985. Frost deterioration may as well have contributed to the cracking in the most water-exposed parts of the deck. The increase in damages from location A to location C is not so easy to explain by exposure conditions only. Structural aspects as internal tensions and shear stresses caused by the expansions in the beams/deck, may contribute to this situation.

Internal cracking:

Plane-polished sections give a highly valuable insight in the internal situation in ASR-damaged concrete. In this project, the extent of cracks in plane-polished sections was classified based on subjective evaluations. No manual crack counting or automatic image analysing was performed. There is, however, a need for easier methods for quantifying the internal crack extent. Work is going on at SINTEF [6] to evaluate existing methods and either optimize existing methods or develop new techniques. These studies are carried out in cooperation between SINTEF and the Laval University in Canada. Concrete/plane-polished sections from the Elgeseter bridge are among several cases involved.

6 CONCLUSIONS

The results from the examinations on the Elgeseter bridge show: 1) The circular columns have vertical surface cracks, most pronounced at the western columns and the western faces (rain and sun loaded). The crack widths increase from the upper part of the columns to the lower part. Surface crack indexes, calculated along the circumference in the mid height of the columns in axis 4 (2014), varies from 3.1 ‰ on the western column to 1.6 ‰ on the corresponding eastern column. 2) The water content in the columns are highest near the western face of the western column, i.e. close to 98 % DCS, decreasing to approximately 70-75 % DCS in the outer 50 mm of the eastern surfaces of both the western and eastern column. 3) The original membrane on top of the bridge deck was defect near the edge beam, due to previous extension of the sidewalk area. Both the water content and the internal crack extent were higher in areas with broken membrane (98-99 % DCS) than in the middle part of the bridge (79-97 % DCS), in depth 0-150 mm from the concrete surface. 4) Internal cracks tend to orientate in a surface parallel direction, both in the columns and the deck.

The results from previous (1995-2011) and later (2014-2015) examinations show a good correlation between the moisture content in the concrete and damage/external and internal cracking, but a relation between RH and DCS is so far not established. Both moisture content and expansions/cracking are highest in structural elements exposed to western weather (rain and sun).

Previous visual observations and analyses on thin and plane-polished sections have revealed more advanced ASR in the outer beams versus the inner beams, and wide single cracks in some of the inner beams. The cracks in the inner beams are related to the load situation (including extra loads from the expansion) and the structural design of the superstructure [8]. The deck had increased damages (delamination) near the joint in axis 10, partly caused by internal tensions and shear stresses due to expansion of the superstructure.

The crack pattern and intensity serve as input to ongoing structural assessment of the superstructure. Further work is going on in a SINTEF project [6] in order to quantify the internal cracking in plane-polished sections, estimate the alkali content in the concrete and find a direct relation between the measured DCS and RH in the drilled cores.

7 REFERENCES

1. Jensen, V: Elgeseter bridge in Trondheim damaged by alkali silica reaction: Microscopy, expansion and relative humidity measurements, treatment with monosilanes and repair, 9th Euroseminar on Microscopy Applied to Building Materials, 9-12th September 2003.
2. Thorenfeldt, E V: Alkali-silica reactions – Strengthening of bridge columns by use of CFRP. Field-testing on Elgeseter bridge 2003-2011, NPRA report No. 339, 2015 (in Norwegian).
3. Aas-Jakobsen (2012): Report from special survey 2012 (in Norwegian).
4. Jensen, V: Elgeseter bridge: Humidity and expansion measurements up to 24. October 2011. Evaluation of humidity, expansion and surface treatments and crack development in un-treated columns. NBTL report No R11257, 2011 (in Norwegian).
5. Jensen, V: Relative Humidity Measured by Wooden Stick Method in Concrete Structures: Long Term Measurements and Reduction of Humidity by Surface Treatment, 6th Int. Conf. on Durability of Concrete, ACI/CANMET, Thessaloniki, Greece 2003 (modified paper)
6. SINTEFs R&D project 236661 «Alkali-silica reaction in concrete – reliable concept for performance testing», (2014-2018). Funded by the Norwegian Research Council and Norwegian industrial partners.
7. Relling, R. H (1999): Coastal Concrete Bridges. Moisture State, Chloride Permeability and Aging Effects. PhD thesis at NTNU, Trondheim, Norway
8. Stemland H.: Structural consequences of ASR in concrete bridge superstructures, NPRA report, 2016 (in Norwegian)
9. Haugen, M.: Laboratory examinations of concrete cores drilled from Elgeseter bridge. SINTEF test report no. 7752-8, 2015 (in Norwegian)
10. Lindgård, J, Rodum, E and Pedersen, B: Alkali-Silica Reactions in Concrete – Relationship between Water Content and Observed Damage on Structures. The Seventh CANMET/ACI International Conference on Durability of Concrete, Montreal, Canada, May 28 - June 3, 2006
11. Lindgård, J, Haugen, M, Skjølsvold, O, Hagelia, P and Wigum, B J: Experiences from evaluation of degree of damage in fluorescent impregnated plane polished sections of half-cores based on the "Crack Index Method", 12th ICAAR Conference, Beijing, October 2004. pp. 939-947

TABLE 1: Surface crack indexes [‰] measured on the columns, 1 m above steel sleeve, 1999 and 2011.

Axis	**1999**				**2011**			
	C1	**C2**	**C3**	**C4**	**C1**	**C2**	**C3**	**C4**
2	2.5	1.0	0.8	1.2	-	-	1.7	1.4
3	2.0	0.9	1.1	0.9	3.3	1.4	1.6	1.3
4	2.4	1.1	1.8	1.5	3.9	2.0	2.7	2.6
Avg 2-4	*2.3*	*1.0*	*1.2*	*1.2*	*3.6*	*1.7*	*2.0*	*1.8*
5	4.5	2.0	1.3	1.0				
6	4.0	3.0	1.7	1.5				
7	1.8	1.6	1.5	1.6				
8	2.7	1.3	0.8	0.5				
9	2.2	1.8	1.5	1.6				
Avg 2-9	*2.8*	*1.6*	*1.3*	*1.2*				

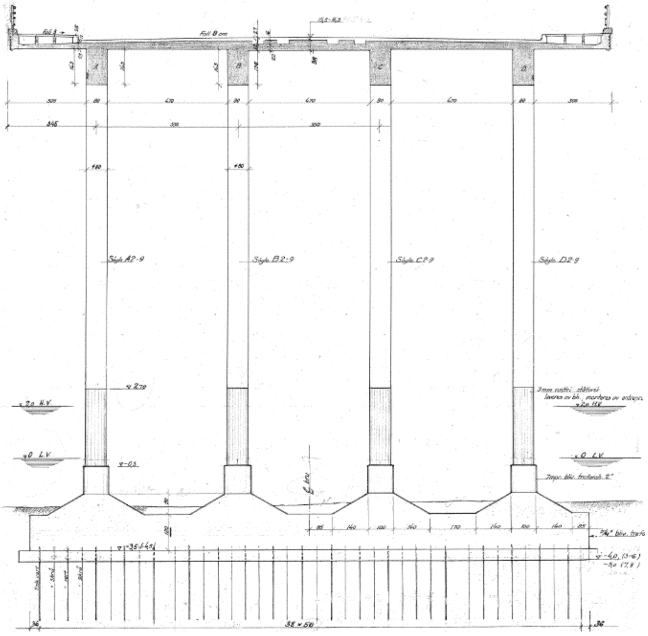

FIGURE 1: Cross section through bridge deck and beams. Columns, ice protection sleeves, foundations and piles.

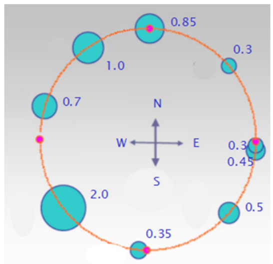

FIGURE 2: Crack widths measured around column 1 in axis 2, in 2011 [4].

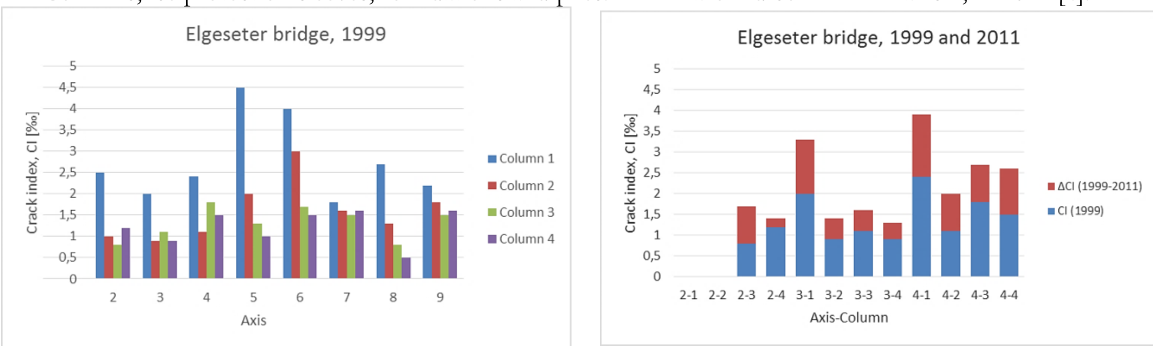

FIGURE 3: Surface crack indexes measured on columns, in level approx. 1 m above the ice protection sleeve [4]. To the left crack indexes measured for all columns in 1999, to the right the crack indexes measured for columns in axis 2-4, given as SCI_{1999} + increase in SCI from 1999 to 2011 ($\Delta SCI_{1999\text{-}2011}$).

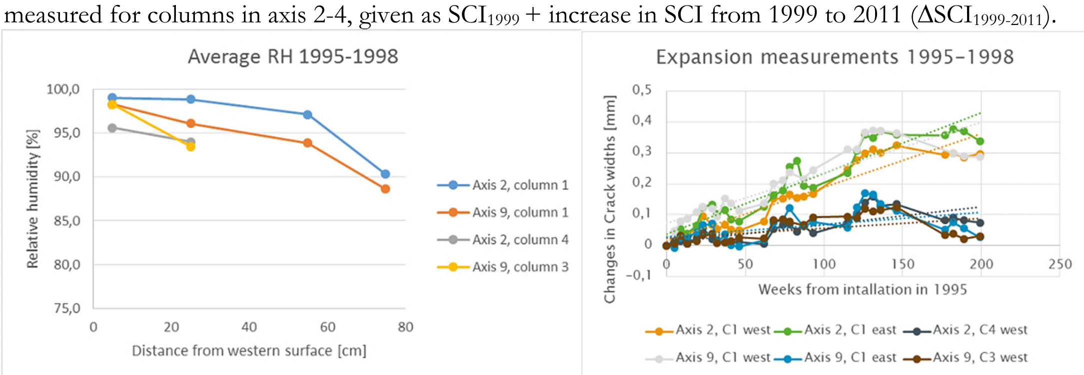

FIGURE 4: To the left: Relative humidity measured with the wooden stick method [5] in columns in axis 2 (column 1 and 4) and axis 9 (columns 1 and 3). Average values of 5-10 yearly measurements from February 1995 to December 1998. To the right: Expansion measurements over single cracks [4].

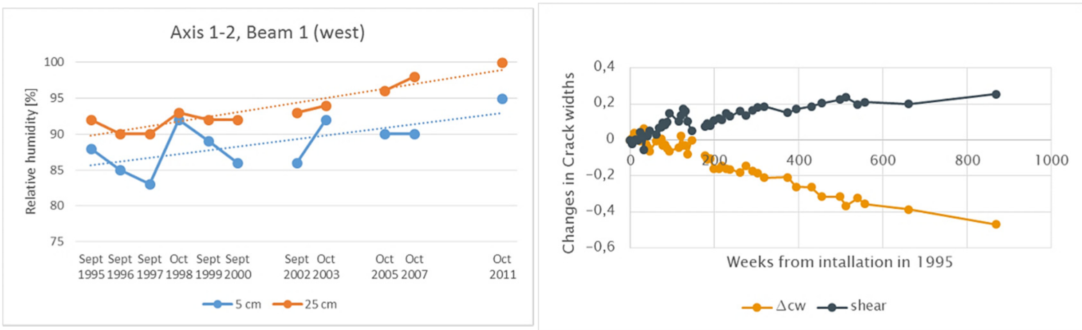

FIGURE 5: To the left: Relative humidity measured with the wooden stick method [5] in west face of western beam between axis 1 and 2, in depths 5 and 25 cm from surface. [4]. To the right: Expansions over the crack (Δcw) and along the crack (shear) [4].

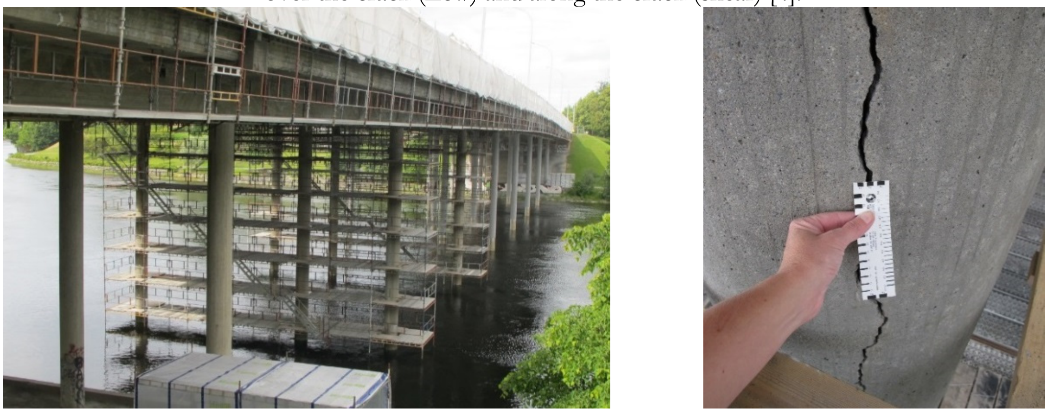

FIGURE 6: Left: Scaffolding raised in axes 3 (nearest) and 4. Surface crack indexes were measured and cores drilled in axis 4, approx. 4.5 m above ice protection sleeve (platform level 3). Right: Maximum crack widths on western side of column 1 in axis 3 were measured on each platform level. Crack width = 7 mm at level 2.

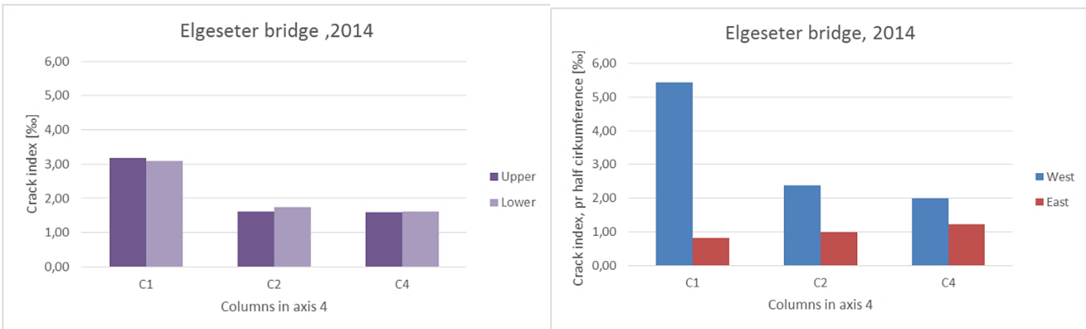

FIGURE 7: Surface crack indexes measured in two levels (internal distance 0.6-0.9 m) of the columns 1, 2 and 4 in axis 4. To the left single values for two lines (upper, lower), to the right crack indexes calculated separately for the two half circumferences (west, east), based on average values for the two measuring lines.

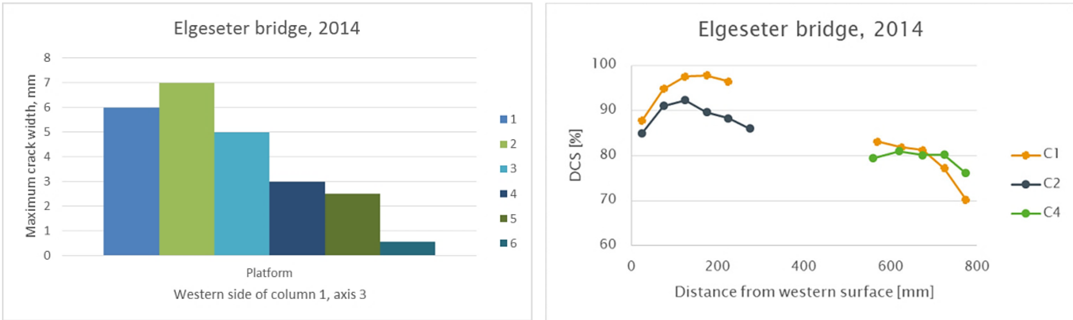

FIGURE 8: To the left: Maximum crack widths on western side of column 1 in axis 3, on different platforms above the river. To the right: Water content, as DCS-profiles, in column 1, 2 and 4 in axis 4 [9].

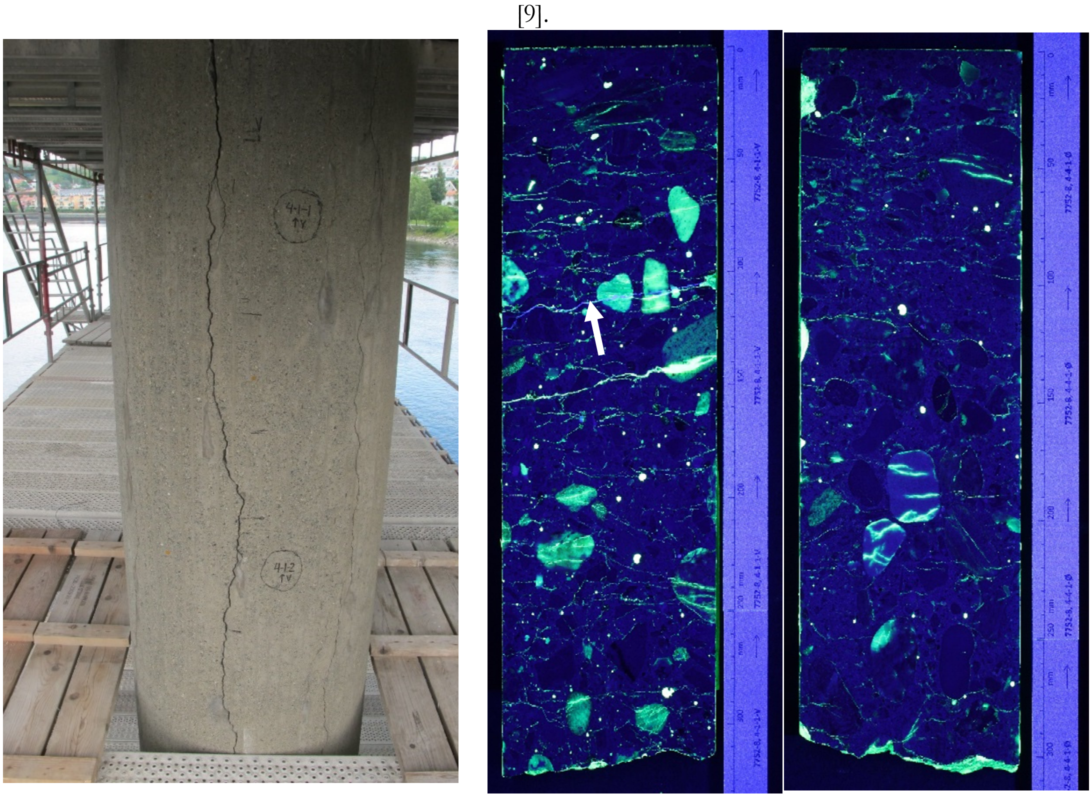

FIGURE 9: Left picture: The west face of the western column (C1) in axis 4, with location for coring marked on the surface. Large vertical crack, measured to 4 mm. Surface crack indexes are measured in two levels corresponding with the core locations. Average SCI for the two lines is 3.1 ‰. Right pictures [9]: Plane-polished sections from west side of column C1 (left) and east side of column C4 (right). C1 is delaminated in depth 110 mm (white arrow) and severely cracked in depth 150 mm. In addition, several fine cracks parallel to the surface. C4 has much less and finer cracks, mainly with surface parallel orientation.

FIGURE 10: Left picture: The western part of the underside of bridge deck. White precipitation are visible from the cantilever and beyond the western beam, indicating severe defects in the membrane in these parts [3]. Right picture: Top of column in axis 9. Previous deflection of columns is visible on the beam. The column top is moved approx. 150 mm.

FIGURE 11: The eastern part of the bridge deck after removing the asphalt, membranes etc. Notches for former tramcar rails were filled with concrete (near the traffic barrier). The right picture shows fracture pieces from upper parts of the concrete deck with clear signs of ASR (white reaction rims).

FIGURE 12: The left picture show the western part of the bridge deck after removing delaminated concrete near the joint. The right picture show the mid/eastern part of the deck near the joint, after repair.

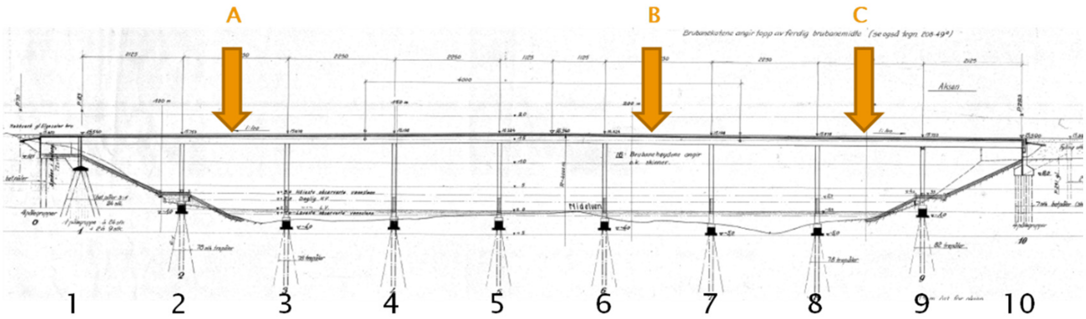

FIGURE 13: Coring locations in the bridge deck given on a longitudinal section. Axis 1 to the left (south). Eight cores were drilled from each location, see FIGURE 14.

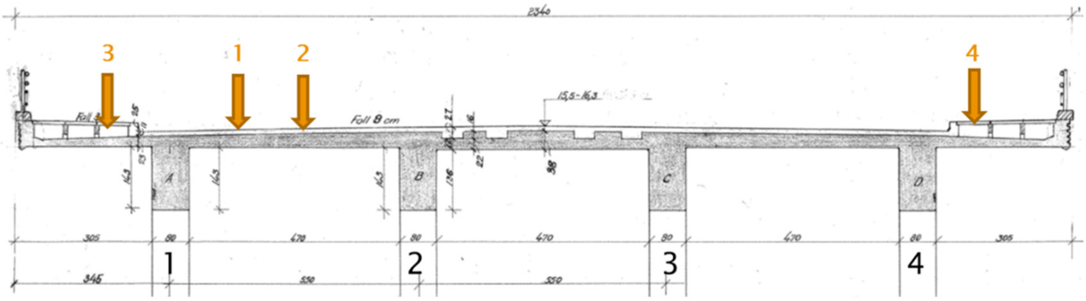

FIGURE 14: Coring locations in the bridge deck given on a cross sectional drawing. Two parallel cores were drilled from each location.

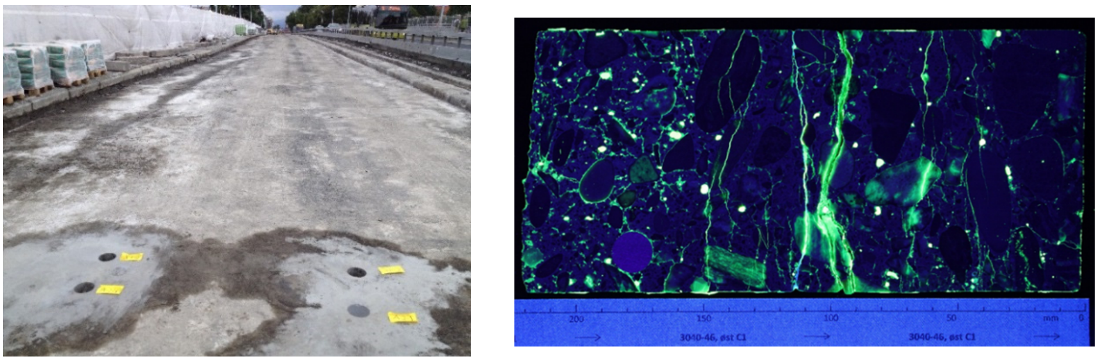

FIGURE 15: The left picture show the coring locations A-1 and A-2, two cores per location. The right picture (photo: SINTEF) show the plane-polished section from location C-4, from top surface (to the right) through the deck (thickness 220 mm). Delaminated in depth 100 mm, several cracks parallel to the surface.

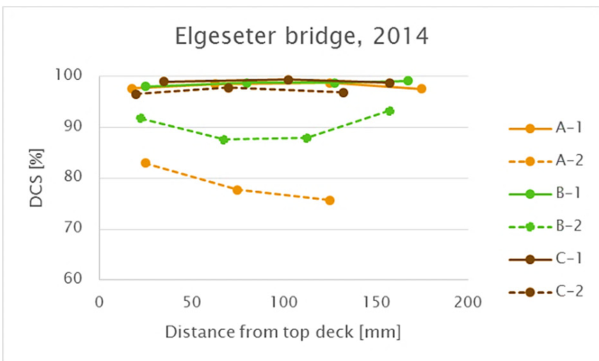

FIGURE 16: DCS profiles measured in the bridge deck. Water content is increasing from location A to C and from location 1 to 2.

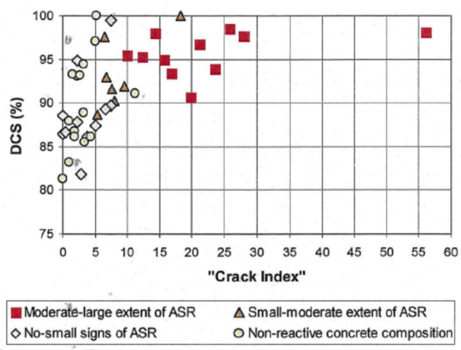

FIGURE 17: DCS versus extent of crack in cores drilled from 46 structures (mainly bridges), described by Crack Index [11]. [10]